

Bias in Polarization CLEAN Imaging

MORGAN HIMES^{1,2}

¹*National Radio Astronomy Observatory*

1003 Lopezville Rd

Socorro, NM 87801, USA

²*University of Florida*

ABSTRACT

Various deconvolution algorithms, such as Hogbom CLEAN, have been developed to construct radio images of the sky. The algorithms used for synthesis imaging in CASA are not robust for polarization imaging of sources with nonzero rotation measures. This project focuses on linear polarization in Stokes Q and U and the bias introduced in cleaning linearly polarized sources. We propose a hybrid method of cleaning based on QU fitting to reduce this bias. This method acquires a fit for a source’s spectral index, polarization angle, Stokes I amplitude, polarized fraction, and rotation measure from a dirty image and uses these parameters to form a model that is fed into CASA for cleaning. Preliminary results show that this method cleans faster than the existing CASA task but introduces some degeneracies that prevent the full polarization information of a source from being recovered.

1. INTRODUCTION

The electric field vector of polarized electromagnetic waves traces an ellipse as a function of time which can be characterized in a Cartesian basis. This ellipse contains the information about the polarization state of the wave. The electric field vector can be written as

$$\mathbf{E} = E_x \hat{\mathbf{e}}_x + E_y \hat{\mathbf{e}}_y = A_x \cos(2\pi\nu t + \delta_x) \hat{\mathbf{e}}_x + A_y \cos(2\pi\nu t + \delta_y) \hat{\mathbf{e}}_y$$

where A_x, A_y are the constant amplitudes and $\delta_y - \delta_x$ is the phase difference. When the phase difference is zero, the wave is linearly polarized. Rewriting E_x, E_y to be real yields

$$E_x = \Re\left\{A_x e^{2\pi i\nu t}\right\} \quad \text{and} \quad E_y = \Re\left\{A_y e^{i(\delta_y - \delta_x)} e^{2\pi i\nu t}\right\}.$$

This polarization state can be described in units of power by the Stokes parameters: I, Q, U, and V. I is total intensity, Q and U are linear polarization, and V is circular polarization. For a monochromatic wave, given the above electric field vector equations, these Stokes parameters are

$$\begin{aligned} I &= A_x^2 + A_y^2 = \langle E_x E_x^* \rangle + \langle E_y E_y^* \rangle \\ Q &= A_x^2 - A_y^2 = \langle E_x E_x^* \rangle - \langle E_y E_y^* \rangle \\ U &= 2A_x A_y \cos(\delta_y - \delta_x) = \langle E_x E_y^* \rangle + \langle E_y E_x^* \rangle \end{aligned}$$

$$V = -2A_x A_y \sin(\delta_y - \delta_x) = -i \left(\langle E_x E_y^* \rangle - \langle E_y E_x^* \rangle \right)$$

such that $I^2 = Q^2 + U^2 + V^2$. For quasi-monochromatic waves, the Stokes parameters are averaged over time and frequency. Stokes parameters in radio interferometry are the inverse Fourier transform of the Stokes visibilities observed by radio telescopes. This project focuses on linear polarization and defines complex polarization as $P=Q+iU$. The above equations and information are attributed to [Brentjens \(2018\)](#).

Propagation of an electromagnetic wave through a magnetized plasma causes Faraday rotation, a wavelength-dependent rotation of the polarization position angle of a linearly polarized wave. Due to birefringence, the left and right circularly polarized components of the wave propagate at different speeds and wavelengths ([Jackson 1962](#)). Faraday rotation can be described by the equation

$$\chi(\lambda^2) = \chi_0 + \text{RM}\lambda^2 \quad \text{where} \quad \text{RM} = \frac{\partial \chi}{\partial \lambda^2}.$$

Here, χ is the polarization position angle, χ_0 is the polarization angle at zero wavelength, and λ is the observing wavelength. The rotation measure RM is sometimes replaced with the more general quantity of Faraday depth, ϕ , defined as

$$\phi = 0.812 \int_{\text{source}}^{\text{observer}} n_e \mathbf{B} \cdot d\mathbf{l}$$

([Heald 2009](#); [Brentjens 2018](#)). A positive Faraday depth indicates a magnetic field pointing in the direction of the observer ([Heald et al. 2009](#)). It is especially important to consider the effects of Faraday rotation at low frequencies and long wavelengths due to the λ^2 dependence of the rotation.

Rotation measure synthesis, implemented by [Brentjens & de Bruyn \(2005\)](#), is a technique used to improve polarimetric observations that can recover low-level polarized flux by splitting up the observing bandwidth into narrow frequency channels. Two equations define the RM synthesis technique:

$$\tilde{F}(\phi) \approx K \sum_{c=1}^N \tilde{P}_c e^{-2i\phi(\lambda_c^2 - \lambda_0^2)} \quad \text{and} \quad R(\phi) \approx K \sum_{c=1}^N W_c e^{-2i\phi(\lambda_c^2 - \lambda_0^2)}$$

Here, the Faraday dispersion function $F(\phi)$ expresses the intrinsic polarized flux in terms of the Faraday depth, and $R(\phi)$ is the RM spread function (RMSF). The convolution of the Faraday dispersion function and RMSF is $\tilde{F}(\phi)$. \tilde{P} is the observed polarized emission, and W is a window function that is zero everywhere except for at values of λ^2 sampled by the telescope. The quantity K is defined as the inverse of the integral over W . The quantity λ_0^2 is ideally the mean of the λ^2 values sampled by the telescope weighted by W . Finally, the index c of the sum denotes the telescope's individual frequency channels used for observing the polarized flux. Performing RM synthesis allows for the recovery of low-level polarized flux and separation of polarized sources along a single line of sight to recover emission at multiple Faraday depths ([Heald 2009](#)).

To construct an image of the sky, a deconvolution algorithm must be used. Most often, this algorithm is a variation of CLEAN. The simplest version is the Hogbom CLEAN algorithm ([Högbom 1974](#)). First, the true image is convolved with the point spread function (PSF) to create a dirty image which is then copied to the residual image. The maximum pixel value and location of the maximum is located and subtracted from the residual image after being multiplied by a gain factor

and the PSF. The flux subtracted and position are then recorded in the model image. The algorithm continues to subtract flux from the residual and add it to the model until reaching a specified number of iterations or a stopping threshold. Then, the model image is convolved with a restoring beam and added to the remainder of the residual image to create a restored image.

Image reconstruction in CASA (McMullin et al. 2007) consists of major and minor cycles. The major cycle uses the Fast Fourier Transform (FFT) and inverse Fast Fourier Transform (iFFT) to transform between the data and image domains. The minor cycle is the deconvolver that operates in the image domain. The major and minor cycle together comprise a χ^2 minimization process that produces a cleaned image .

Hogbom CLEAN in CASA treats each frequency channel as an individual image, such that a measurement set with n channels would produce a cube of n images. Multi-Term Multi Frequency Synthesis, in contrast, makes a single wideband image. Neither Hogbom CLEAN nor MTMFS are robust for polarization imaging for sources with nonzero rotation measures. This project will suggest a hybrid method to fit for the polarized structure of the source based on the process of QU fitting.

This hybrid method is necessary to address CLEAN's inadequacies in imaging for linear polarization. Particularly, CLEAN introduces a bias in cleaning sources with nonzero rotation measures. The stopping threshold of Hogbom CLEAN introduces a bias because there is source flux below the noise level that does not get cleaned and is not added back to the model image. This prevents achieving a full understanding of the source's polarization state. For sources with a rotation measure, the quantities

$$Q = P \cos(2\chi) \quad \text{and} \quad U = P \sin(2\chi)$$

can be under the noise level, zero, or even negative. Polarized intensity P is positive, so even if the true Stokes parameters are zero, P will yield a non-zero estimate in the presence of noise. Modeling polarized intensity $P=Q+iU$ is a possible way to reduce this bias.

QU fitting is a well-studied method equivalent to rotation measure synthesis in RM space. It has been shown by O'Sullivan et al. (2012) to work for complex structures in the image domain and can be used to model cases with depolarization mechanisms. The complex polarized signal is modeled by the equation

$$P = p_0 I_0 e^{2i(\chi_0 + \text{RM}\lambda^2)} \quad \text{where} \quad I \propto \nu^\alpha.$$

Here, p_0 is the fractional polarization and χ_0 is the polarization position angle made by the electric field vector. Fractional linear polarization p can be defined by the equation

$$p = \sqrt{Q^2 + U^2}.$$

This project's simulations vary the free parameters p_0 , χ , and RM. I_0 is changed through varying the spectral index α . QU fitting is then used to estimate an initial model for cleaning (see 2).

The main goals of the project were to create realistic simulations of different types of polarized sources, characterize the bias in Stokes Q and U from the simulations, and propose a method for reducing this bias.

2. METHOD

The procedure was conducted in two steps: simulating and fitting. The first task for simulating realistic sources was the creation of measurement sets. The measurement sets were created with

information from the Very Large Array (VLA) in D configuration where the maximum antenna separation is about 1 km. The measurement sets were created with 16 spectral windows with 64 channels each totaling 1024 channels from 2.048 to 4.096 GHz in steps of 0.002 GHz, corresponding to the VLA’s S-Band. The simulations were built with S-Band frequencies because the resulting models are informative for showing the kind of polarized science that can be done with VLASS, an all-sky radio survey that has full linear Stokes polarimetry at S-Band frequencies (Lacy et al. 2020).

After the creation of the measurement set, the source was added to a blank image and copied back to the measurement set which was then corrupted with noise. Wideband point sources with varying spectral indices, rotation measures, and polarization position angles were simulated with different levels of noise. The simulations were focused on point sources because they can be characterized by their phases and amplitudes, making the early stage results of the project simpler to interpret. The spectral indices of the sources were varied because spectral index is the dominant term in spectral behavior of the source flux density.

Two different rotation measure values were used for the simulations: 0 and 25. Modeling sources with no rotation measure was important to incorporate as the simplest case in the simulation to serve as a comparison for more complicated simulations. A rotation measure of 25 was chosen for the other sources because it is approximately the median rotation measure out of the galactic plane (Taylor et al. 2009). For high rotation measure sources, modeling with limited frequency coverage is difficult.

These simulations were largely conducted through the use of two python scripts: `simulate_ms.py` and `make_images.py`. The class `MakeSource` of `simulate_ms.py` contains functions for setting up source and field information and adding sources to a blank image. The other class `SimulateMS` constructs the empty measurement set with a chosen observation setup. The class `MakeImage` of `make_images.py` has functions that can add noise to a measurement set, make an initial dirty image with a source, make a cleaned verification image, and test the background distribution of an image for noise. See 3 for more detail.

A QU fitter, `fitter.py`, was created for the fitting step of the procedure. The fitter sets initial Q and U values as

$$Q = pI \cos(2(\chi_0 + RM\lambda^2)) \quad \text{and} \quad U = pI \sin(2(\chi_0 + RM\lambda^2)).$$

The function `getqupix` takes the image name and pixel location and returns the pixel values and the range of frequencies in the image (see 3). These are then fed into astropy’s (Astropy Collaboration et al. 2013, 2018) `LevMarLSQFitter` which uses the Levenberg-Marquardt algorithm and least squares statistic.

After simulating the sources, the fitter was applied to the dirty image to fit the Stokes I amplitude, polarization angle, rotation measure, and spectral index. Then the model image was updated with the fit values, and a new residual was computed and used for cleaning. This takes the initial guess and moves it closer to the true value faster than Hogbom CLEAN. The information across 1024 pixel values in all channels is compressed to 4 fit values. A single time window was used in cleaning to demonstrate that the method works in situations with high noise and low signal.

3. CODE OVERVIEW

A number of class objects were created to perform the simulation and fitting. The class `MakeSource`, of `simulate_ms.py`, contains several methods that simulate sources and add them to images. The

method `makeSource` sets up source and field information, and it should be called several times for different pointings and locations. The other three methods in `MakeSource` are `pointSource`, `makeWidebandSource`, and `makeMultipleWidebandSources`. The first, `pointSource`, is the simplest that adds a point source with Stokes I, Q, U, and V values defined to a single frequency channel of a model image given a single flux, polarized intensity, and polarization angle. The method `makeWidebandSource` adds a point source to several frequency channels of a model image. Unlike the single channel case, this method requires a polarized intensity, polarized angle, spectral index, and rotation measure. The method currently uses the center of the band as a reference with a reference frequency of 1 Jansky, but this could be expanded to take any reference flux and frequency. The method `makeMultipleWidebandSources` performs the same as `makeWidebandSource` but takes a dataframe that contains the polarized intensity, polarized angle, spectral index, rotation measure, and position of every source being added. These sources are all added to several channels of a model image.

The class `SimulateMS`, also of `simulate_ms.py`, builds an empty measurement set with a specified observing setup, including antenna configuration, phase center direction, spectral windows, date, timerange, and other metadata. This is done with the method `makeMSFrame`. First, the antenna configuration is set; the configuration can be a real or fictitious telescope. Then, the polarization mode and spectral windows are set. This portion can be called multiple times with different names to allow for multiple polarization modes and spectral setups. The source and field information are drawn from the `makeSource` method of the `MakeSource` class. The elevation limits and integration time are then set and the MS metadata is constructed.

Once the measurement set is constructed, the source can be simulated and added to the MS. The class `MakeImages`, of `make_images.py`, carries out this task. The method `makeInitialImageSource` from `MakeImages` first uses `makeMSFrame` from `SimulateMS` to generate a new blank measurement set with the preferred observing setup. CASA's `tclean` is then used to create a blank source image from the measurement set. Depending on the type of source, `pointSource`, `makeWidebandSource`, or `makeMultipleWidebandSources` are used from `MakeSource` to add the simulated source to the blank model image. Next, `tclean` is run again to save the predicted model visibilities in the model data column. The model column is then copied to the data column for imaging.

The method `addNoise` can then be used to corrupt the measurement set with noise. This requires the existence of a noise measurement set that does not contain a source. These measurement sets were constructed by simply creating a blank measurement set with `makeMSFrame` and adding noise to the measurement set. The method `addNoise` takes the noise-only measurement set and adds it to the source measurement set. If desired, the method `makeVerificationImage` can be used to run `tclean` and create a cleaned image of the source.

The QU Fitter, stored in `fitter.py`, contains three functions for performing the fits. The first two, `qfit` and `ufit`, take the Stokes I amplitude, polarized fraction, source angle, and rotation measure and return the initial Q and U values obtained from the equations described in section 2. The next function, `getqupix` takes the image name and position of the source. It then stores the pixel values of Stokes Q and U from the image in the given position. It also stores the range of frequencies spanned by the channels of the image provided. The function then returns these frequencies and pixel values.

The script `fitter.py` then establishes the `LevMarLSQFitter` of `astropy` as the fit function. For the Q fit, the fitter takes the initial Q value from `qfit` and the frequency and pixel values from `getqupix`

to return an estimate for the Stokes I amplitude, spectral index, rotation measure, polarized fraction, and source angle. The U fit operates similarly but takes the initial U value from `ufit`. In practice, the fitter should be run on the dirty image and applied to the model image. The model image should then be used for cleaning. The model can be iteratively updated in this way as the cleaning proceeds.

4. RESULTS AND DISCUSSION



Figure 1. The QU fitting process was applied to a source with $\alpha = 0$, $RM = 0$, and $\chi_0 = 22.5$. The figure shows the result of the fitting in Q (left) and U (right) for one spectral window (2.048-2.176 GHz). The results of the QU fit are shown in blue, Hogbom CLEAN in green, and the true values of Q (left) and U (right) in red. Noise of $\approx 10\sigma$ is applied to the true Q and U values.



Figure 2. As in Figure 1, the QU fitting process was applied to the same source with $\alpha = 0$, $RM = 0$, and $\chi_0 = 22.5$. The figure shows the result of the fitting in Q (left) and U (right) for all spectral windows (2.048-4.096 GHz). The results of the QU fit are shown in blue, and the true values of Q (left) and U (right) are shown in red. The Hogbom CLEAN estimate is not shown, but performs similarly to the case in Figure 1. As in Figure 1, noise of $\approx 10\sigma$ is applied to the true Q and U values.

Table 1. QU Fit for $\alpha = -0.5$, RM = 25 Source

Fit	I_{amp} (Jy)	Polarized Fraction p (Jy)	Source Angle χ_0 (deg)	RM (rad/m/m)	Spectral Index α
Q Fit	0.89986956	0.04499348	28.09828851	-31.18463698	-0.48250341
U Fit	1.04251471	0.05212574	8.25222089	11.015855	-1.01194633
True Model	1.0	0.05	22.5	25	-0.5

For the case where the source has no rotation measure, no spectral index, and $\chi_0 = 22.5$, it can be seen that the QU fitting model reaches the answer faster than Hogbom CLEAN (see Figure 1). The QU fitting method is seen to underestimate in Q and overestimate in U for the first spectral window. As the bandwidth is increased, it can be seen that basing the fit values on the first channel influences the fit up or down (see Figure 2).

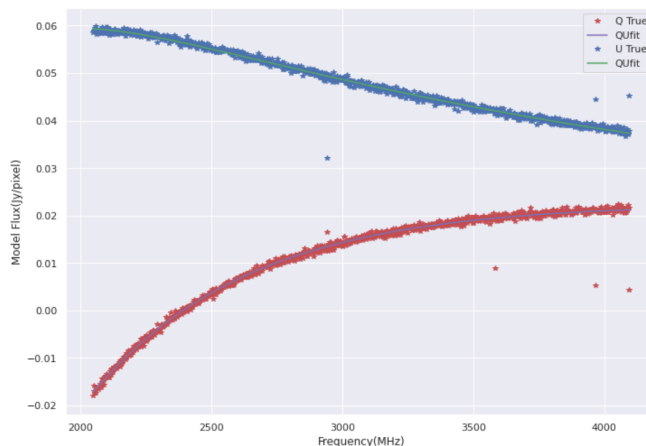


Figure 3. The QU fitting process was applied to a source with $\alpha = -0.5$, RM = 25, and $\chi_0 = 22.5$. The figure shows the result of the fitting in Q and U for all spectral windows (2.048-4.096 GHz). The true values of Q are shown in red, and the true values of U are shown in blue. The QU fit to Q is shown as a green line, and the QU fit to U is shown as a purple line. Noise of $\approx 5\sigma$ is applied to the true Q and U values.

For the case where $\alpha = -0.5$, RM = 25, and $\chi_0 = 22.5$, the fitter models the curve well (see Figure 3). Upon further inspection, however, the fitter’s estimates of the source angle, rotation measure, and spectral index do not necessarily match the inputs used to simulate the source (see Table 1). This suggests that a combination of these three parameters causes a degeneracy. Multiple combinations of these parameters could produce the same fit to the data.

5. FUTURE STEPS

There are many ways in which the current project could be expanded upon. The fitter was built using least squares fitting, but it could be improved by incorporating a goodness of fit test instead. Joint minimization of $Q+iU$ instead of Q and U separately could also help solve the degeneracy issue. RM synthesis could also be implemented to solve the degeneracy issue, but it is computationally

expensive. Implementing a loop gain similar to that of Hogbom CLEAN into the fitting could also improve the fit quality.

It is also worth considering that while the proposed method is much faster than Hogbom CLEAN for small image size (B, C, and D configurations of the VLA), computing time scales as n^2 where the image size is $n \times n$ pixels. If information about Stokes I is known, it can be incorporated to improve fit quality and speed.

Another future step would be to expand the method to non-point sources and fields with multiple sources. A single field with, for instance, a hundred sources would introduce unique challenges in cleaning that are not identified or addressed by the single source case.

Finally, the ultimate goal is to integrate the fitting process directly into CASA's `tclean` task.

This project was primarily supported by the National Science Foundation (NSF) as part of an REU experience in collaboration with the National Radio Astronomy Observatory. I gratefully acknowledge the support of the National Radio Astronomy Observatory and NRAO staff for this project. I would like to thank Dr. Preshanth Jagannathan for his guidance in the research process, and I would also like to acknowledge Dr. George Heald for his contributions to the research objectives.

Software: CASA (McMullin et al. 2007), Astropy (Astropy Collaboration et al. 2013, 2018), Matplotlib (Hunter 2007), Seaborn (Waskom 2021)

REFERENCES

- Astropy Collaboration, Robitaille, T. P., Tollerud, E. J., et al. 2013, *A&A*, 558, A33, doi: [10.1051/0004-6361/201322068](https://doi.org/10.1051/0004-6361/201322068)
- Astropy Collaboration, Price-Whelan, A. M., Sipőcz, B. M., et al. 2018, *AJ*, 156, 123, doi: [10.3847/1538-3881/aabc4f](https://doi.org/10.3847/1538-3881/aabc4f)
- Brentjens, M. A. 2018, in *Astrophysics and Space Science Library*, Vol. 426, *Astrophysics and Space Science Library*, 159, doi: [10.1007/978-3-319-23434-2_10](https://doi.org/10.1007/978-3-319-23434-2_10)
- Brentjens, M. A., & de Bruyn, A. G. 2005, *A&A*, 441, 1217, doi: [10.1051/0004-6361:20052990](https://doi.org/10.1051/0004-6361:20052990)
- Heald, G. 2009, in *Cosmic Magnetic Fields: From Planets, to Stars and Galaxies*, ed. K. G. Strassmeier, A. G. Kosovichev, & J. E. Beckman, Vol. 259, 591–602, doi: [10.1017/S1743921309031421](https://doi.org/10.1017/S1743921309031421)
- Heald, G., Braun, R., & Edmonds, R. 2009, *A&A*, 503, 409, doi: [10.1051/0004-6361/200912240](https://doi.org/10.1051/0004-6361/200912240)
- Högbom, J. A. 1974, *A&AS*, 15, 417
- Hunter, J. D. 2007, *Computing in Science & Engineering*, 9, 90, doi: [10.1109/MCSE.2007.55](https://doi.org/10.1109/MCSE.2007.55)
- Jackson, J. D. 1962, *Classical Electrodynamics*
- Lacy, M., Baum, S. A., Chandler, C. J., et al. 2020, *PASP*, 132, 035001, doi: [10.1088/1538-3873/ab63eb](https://doi.org/10.1088/1538-3873/ab63eb)
- McMullin, J. P., Waters, B., Schiebel, D., Young, W., & Golap, K. 2007, in *Astronomical Society of the Pacific Conference Series*, Vol. 376, *Astronomical Data Analysis Software and Systems XVI*, ed. R. A. Shaw, F. Hill, & D. J. Bell, 127
- O’Sullivan, S. P., Brown, S., Robishaw, T., et al. 2012, *MNRAS*, 421, 3300, doi: [10.1111/j.1365-2966.2012.20554.x](https://doi.org/10.1111/j.1365-2966.2012.20554.x)
- Taylor, A. R., Stil, J. M., & Sunstrum, C. 2009, *ApJ*, 702, 1230, doi: [10.1088/0004-637X/702/2/1230](https://doi.org/10.1088/0004-637X/702/2/1230)
- Waskom, M. L. 2021, *Journal of Open Source Software*, 6, 3021, doi: [10.21105/joss.03021](https://doi.org/10.21105/joss.03021)